MITSUBISHI ELECTRIC RESEARCH LABORATORIES
http://www.merl.com

Orthogonality Factor in WCDMA Downlinks in Urban Macrocellular Environments

Neelesh Mehta, Andreas Molisch, Larry Greenstein

TR2005-100 November 2005

Abstract

Multipath dispersion leads to the loss of orthogonality between signals transmitted simultaneously on a wideband code division multiple access (WCDMA) downlink. The orthogonality factor (OF), which models its impact in the link signal-to-interference-plus-noise ratio (SINR) equation, depends-to a large extent-on the power delay profile of the multipath channel between the mobile and its serving base station. We use the comprehensive and general COST259 channel model for urban cellular environments to evaluate the impact on the OF of multipath clusters and distance-dependence of the multipath delay decay time constant, both of which have been observed in several channel measurements. The observed large standard deviation of the OF indicates that using a single value for all users in downlink capacity analyses and simulations, as has been the practice, may lead to erroneous conclusions. We also propose an empirical model to analytically characterize the observed statistics of the OF.

IEEE Globecom 2005

Orthogonality Factor in WCDMA Downlinks in Urban Macrocellular Environments

Neelesh B. Mehta, *Member, IEEE*, Andreas F. Molisch, *Fellow, IEEE*,
Larry J. Greenstein, *Life Fellow, IEEE*

***Abstract*— Multipath dispersion leads to the loss of orthogonality between signals transmitted simultaneously on a wideband code division multiple access (WCDMA) downlink. The orthogonality factor (OF), which models its impact in the link signal-to-interference-plus-noise ratio (SINR) equation, depends – to a large extent – on the power delay profile of the multipath channel between the mobile and its serving base station. We use the comprehensive and general COST259 channel model for urban cellular environments to evaluate the impact on the OF of multipath clusters and distance-dependence of the multipath delay decay time constant, both of which have been observed in several channel measurements. The observed large standard deviation of the OF indicates that using a single value for all users in downlink capacity analyses and simulations, as has been the practice, may lead to erroneous conclusions. We also propose an empirical model to analytically characterize the observed statistics of the OF.**

I. Introduction

Third generation cellular systems such as wideband code division multiple access (WCDMA) [1] are designed to efficiently handle multiple services such as voice, data, and multimedia applications. WCDMA (Release 5) delivers data rates greater than 10 Mbps.

The spreading codes used in WCDMA are a concatenation of long pseudo-random scrambling sequences and short orthogonal channelization sequences. Multipath dispersion leads to a loss in orthogonality between the spreading codes. This is measured in WCDMA downlink capacity analyses and simulations by the orthogonality factor (OF) [1]–[4]. The lower the OF, the lower the intra-cell interference – an OF of 0 corresponds to no interference and an OF of 1 corresponds to considerable downlink interference.[1] Values between 0.1 and 0.6 are commonly used for the OF [1]–[3]. An increase in the OF can have a significant negative impact on system capacity, and manifests itself in the form of reduced data throughput and fewer voice users per cell.

A complete and accurate characterization of the OF is clearly essential in cell capacity analysis and planning. The value of the OF depends on the channel delay profile, chip pulse shape, the number of Rake fingers in the receiver, etc. The results of [5], [6] show that the channel's delay profile determines the OF to a large extent, while parameters such as the chip pulse shape and the number of Rake fingers play a minor role. Reference [6] established a simple affine relationship between the time-averaged OF and the reciprocal of the diversity factor, which is a measure of the multipath dispersion of the channel.

Several channel measurement analyses have shed light on the variation of the multipath dispersion in a cell. The analysis by Greenstein *et al.* [7] showed that the dispersion encountered in a given environment statistically increases with the distance of the mobile station (MS) from the base station (BS). Furthermore, it is correlated with shadowing [7], [8]. Measurement results also show that in some environments, the multipath components are not always uniformly spread out, but arrive in clusters [9], [10]. Multiple clusters occur in macrocells due to large objects like high-rise buildings or hills, which cause significant power to reach the MS with large excess delays [11]. Thus, the power delay profile, and consequently the OF itself, can be quite different for locations spaced far apart.

Given the close relationship between the power delay profile and the OF, the presence of multiple clusters and the distance of the MS from the BS can significantly affect the OF observed. However, system-level simulations have traditionally used only a handful of pre-specified delay profiles that do not capture the above two phenomena. This paper quantifies the behavior of the OF over the entire urban macrocellular area and measures the impact of the above two phenomena on it.

The dependence of the OF on the distance has been studied before in [12], which also used the Greenstein model. However, it did not take multiple clusters into account. Another difference is that it used the OF formula of [13], which assumes a Rake finger weighting scheme that ignores inter-cell interference and noise, but accounts for the different intra-cell interference seen by different fingers. Also, no model was proposed for characterizing the distribution of the OF over a cell area. Using the same definition of the OF, [13], [14] used ray-tracing simulations over an urban area and observed a high correlation between the logarithm of the OF and the log of the multipath delay decay time constant. However, the variation with distance was not modeled. The studies in [15], [16] used actual channel measurements and observed a wide variability in the time-averaged OF. However, the definition of the OF in [15] seems to be based on the ratio of the fading-

Part of this work was done when all the authors were at AT&T Labs – Research, Middletown, NJ, USA. Neelesh B. Mehta and Andreas Molisch are now at the Mitsubishi Electric Research Labs (MERL), Cambridge, MA, USA. Larry Greenstein is a Research Professor at WINLAB in Rutgers University, NJ, USA. A. F. Molisch is also at the Department of Electroscience, Lund University, Lund, Sweden.

[1]Several authors use an alternate definition of the OF in which a value of 0 corresponds to considerable downlink interference and a value of 1 corresponds to no interference. To maintain consistency, we convert their results to our notation whenever we discuss them.

averaged signal power to the fading-averaged interference plus noise power, which is different from the one considered in this paper. The reader is referred to [5] for a full discussion of the various OF formulae and their fundamental dependence on the SINR modeling assumptions.

While using stored traces or ray-tracing methods leads to very accurate channel descriptions, as they can incorporate all the details of the radio environment, their results are location-specific and can suffer from a lack of generality. We therefore use the comprehensive COST259 stochastic macrocellular channel model, which is among the most general models currently available [17]. The 3GPP spatial channel model (SCM) [18] also borrows from the COST259 model. Using a model such as COST259 that integrates the vast amount of previous published and unpublished work on channel modeling and measurements [7], [8], [19], [20] into a single general framework enables us to make general observations and conclusions about the behavior of the OF in a cellular area.

COST259 includes the above-mentioned Greenstein model and explicitly models multiple clusters. It also models the observed interrelations between the large-scale and small-scale behavior of the channel. COST259 thus provides a systematic method to stochastically generate the experimentally observed power delay profiles encountered over an entire cell. To account for the different terrains in which cells can be located, COST259 specifies two generic urban environments, namely, Generalized Typical Urban (GTU) and Generalized Bad Urban (GBU). GTU describes cities and towns with buildings having mostly homogeneous height and density. On the other hand, GBU describes cities with distinctly inhomogeneous building heights or densities, and is the more dispersive environment. The power delay profiles in GBU have, on an average, close to twice as many clusters than in GTU.

The paper is organized as follows: Section II briefly describes the COST259 channel model for macrocells and the analytical results on the OF that we use in this paper. The statistics of the OF for delay profiles generated from COST259 are presented and analyzed in Section III. Section IV summarizes our findings.

II. Background

A. COST259 Channel Model for Macrocells

COST259 is a parametric stochastic model that characterizes the small-scale and the large-scale behavior of the wireless channel. Compared to previous models like COST207 [21], the COST259 model is significantly more comprehensive since it simultaneously models many of the important parameters of the channel, such as path loss, shadow fading, short-term fading, temporal and angular dispersion, and polarization, and their inter-relationships.

For a given MS location, the power delay profile in COST259 incorporates the effect of multiple clusters and depends on the distance of the MS from the BS as follows:

1) Scatterer Clusters and Visibility Regions: Scatterer clusters, such as buildings and mountains, are distributed over the cell area. Each cluster has multiple "visibility regions" associated with it in the cell. Each visibility region is a circle of radius R_C. An MS located within a cluster's visibility region experiences non-line-of-sight (NLOS) multipath dispersion due to that cluster, and sees it in the form of a multipath cluster in the power delay profile of its channel. The location of the MS thus determines the number of multipath clusters in the channel impulse response.

The probability that a scatterer cluster spawns a visibility region at a distance r from the BS is given by a Gaussian distribution with standard deviation r. The placing of the clusters and their corresponding visibility regions is stochastic and is specified in detail in [17]. In addition, local scattering near the MS always contributes one multipath cluster. As the MS moves, it may enter new visibility regions and leave old ones. Not only does it experience short-term fading, but its small-scale averaged power delay profile also dynamically changes, albeit over larger distances.

A similar mechanism allows for the occurrence of at most one line-of-sight (LOS) component and determines its power [20]. The probability that an LOS component exists decreases linearly with the distance of the MS from the BS; it vanishes beyond a cut-off distance of 500 m and increases as the height of the BS increases.

The multipath components undergo independent, time-correlated Rayleigh fading that depends on the Doppler frequencies. The power of each multipath within a cluster decays exponentially as a function of its relative delay from the first multipath of the cluster. The powers of the clusters also decay exponentially as a function of their excess path delays, where the excess path delay is the delay of the first path of the cluster relative to the first path of the first cluster. However, once the excess path delay exceeds a 10 μsec threshold, there is no further decay in the cluster power. The power distribution as a function of the directional coordinates of the multipath components has also been specified, but is beyond the scope of this paper. The shadowing is specified to be the same for all the multipath components of a cluster, and follows a log-normal distribution. However, it is independent between clusters.

2) Distance-Dependent Delay Decay Constant: The exponential power delay profile, $P_n(\tau)$, of the n^{th} cluster, with initial time offset τ_n, is characterized by the decay time constant, $\sigma_{n\tau}$, as follows:

$$P_n(\tau) = \frac{1}{\sigma_{n\tau}} \exp\left(-\frac{\tau - \tau_n}{\sigma_{n\tau}}\right), \quad (\tau > 0). \tag{1}$$

The decay time constant, in turn, depends on the distance, r, of the MS from the BS as follows:

$$\sigma_{n\tau} = m_{s\tau} \left(\frac{r}{1000}\right)^{\epsilon} 10^{0.1 s_{s\tau} Z_m}, \tag{2}$$

where $m_{s\tau}$ is the median delay decay constant at a distance $r = 1000$ m, $s_{s\tau}$ is the standard deviation expressed in dB, and ϵ is the distance exponent. Z_m is a zero-mean, unit-variance Gaussian random variable that is correlated with the Gaussian random variable used for generating the log-normal shadowing. Thus, the delay decay constant of a cluster is itself a random variable and is correlated with the cluster's shadow

TABLE I

IMPORTANT COST259 PARAMETERS FOR URBAN MACROCELLULAR ENVIRONMENTS

Parameter	**GTU**	**GBU**
Carrier freq. [GHz]	2.0	2.0
BS height [m]	30.0	50.0
MS height [m]	1.5	1.5
Ave. rooftop height [m]	15.0	30.0
Ave. no. of clusters	1.17	2.18
Shadow fading dB standard deviation	6.0	6.0
Median delay decay constant of each cluster ($m_{s\tau}$)	0.4	0.4
Standard deviation of decay constant [dB] ($s_{s\tau}$)	3.0	3.0
Decay constant's distance exponent (ϵ)	0.5	0.5
Shadowing and decay constant correlation	0.5	0.5
Visibility region radius (R_C) [m]	100.0	100.0

fading over the terrain. The values of the parameters for the GTU and GBU environments are listed in Table I.

B. Orthogonality Factor

A general analytical expression for the OF, conditioned on the channel's instantaneous power delay profile, was derived in [5] and was shown to be in excellent agreement with simulation results. It is used in this paper to calculate the instantaneous OF, β_o.

For the special case in which the multipath delays are integer multiples of the chip duration, the formula for the instantaneous OF for a full Rake receiver that can handle all the multipaths, simplifies to:

$$\beta_o = 1 - \frac{\sum_{i=1}^{L} |\alpha_i|^4}{\left(\sum_{i=1}^{L} |\alpha_i|^2\right)^2}, \tag{3}$$

where L is the total number of multipaths and α_i is the fading coefficient of the i^{th} multipath. This expression holds when the Rake finger weights are complex conjugates of the multipath fading coefficients.

In this paper, we study the time-averaged OF, $\overline{\beta}_o$. This is the Monte-Carlo average of the instantaneous OF over the small-scale fading, and is evaluated numerically.

III. OF AND COST259 IMPLEMENTATION AND RESULTS

A. Implementation Details

The recommended set of parameters in [17] was utilized in the implementation of the COST259 model used here. Table I lists the values of some of the relevant parameters for the urban environments we consider in this paper. The radius of the macrocell for both the environments (metropolitan terrain) was chosen as 1 km. The OF was calculated for a rectangular pulse shape and a full Rake receiver (all paths processed). Note that the chip pulse shape and the number of fingers in the receiver have only a marginal impact on the OF [5], making the results in this paper approximately applicable to partial Rake receivers and systems with other chip pulse shapes, as well. While the 2 GHz carrier frequency is used in this study, the qualitative behavior of the OF will be the same for all the carrier frequencies in which the COST29 model is valid.

For a given scatterer and visibility region configuration, the MS location was determined as follows: For a given distance, r, from the BS, the MS was placed at 500 randomly generated locations in the cell. The distances were chosen to be $0.1d, 0.2d, \ldots, 1.0d$, where d is the cell radius. In addition, three different realizations of the scatterer and visibility region placements were used to generate the results. A different set of delay profiles, and consequently the OF, is obtained in each realization. The time-averaged OF, $\overline{\beta}_o$, was computed for each of the delay profiles so generated. In view of the dependence of the delay decay time constant on r, the statistics of $\overline{\beta}_o$ were tabulated as a function of r.

B. Results

Figure 1 plots the median value of the delay decay constant of the first cluster (due to local scattering) and shows its increase with r. Note that it is the same for GTU and GBU.

Figure 2 plots the cumulative distribution function (CDF) of $\overline{\beta}_o$ at each of several distances of the MS from the BS, for the GTU environment. In the same manner, Figure 3 plots the CDF of $\overline{\beta}_o$ for the GBU environment. Notice that, as the distance increases, the CDF of $\overline{\beta}_o$ shifts to the right considerably. This is a consequence of (2), in which the median value of delay decay constant (which itself is a random variable) increases with r. The increased multipath dispersion begets an increase in $\overline{\beta}_o$. Even though GTU and GBU follow the same cluster delay decay constant vs. distance curve in the first cluster, GBU exhibits greater values of the OF due to the presence of more clusters in its power delay profiles (Table I).

C. Distance-Dependent Model for $\overline{\beta}_o$

The CDFs, $F(\overline{\beta}_o)$, of $\overline{\beta}_o$ for GTU and GBU are plotted on a Gaussian probability scale in Figure 4 and Figure 5, respectively. In other words, for an abscissa $\overline{\beta}_o$, we plot $\text{erfcinv}(2(1 - F(\overline{\beta}_o)))$ on the y-axis. This is called a Gaussian probability scale because for a Gaussian distribution with mean μ and standard deviation σ, we have the linear relationship $\text{erfcinv}(2(1 - F(\overline{\beta}_o))) = \frac{\overline{\beta}_o - \mu}{\sqrt{2}\sigma}$. Observe that the plots are nearly (but not exactly) linear. Therefore, for a given r, a Gaussian distribution may be used to approximate the probability distribution of $\overline{\beta}_o$. If $y = p_1(r)x + p_2(r)$ is used as the curve-fitting approximation in these two figures, with y being the ordinate and x the abscissa, then the Gaussian mean and standard deviation of $\overline{\beta}_o$ are given by $\mu(r) = -\frac{p_2(r)}{\sqrt{2}p_1(r)}$ and $\sigma(r) = \frac{1}{\sqrt{2}p_1(r)}$. The minimum RMS curve-fitting error was found to be about 0.10 for $r \geq 200$ m, and was slightly higher (0.17) for $r = 100$ m. That the lines are essentially shifted versions of each other implies that the distribution of $\overline{\beta}_o$ has a distance-dependent mean and a distance-independent standard deviation.

Note that the Gaussian distribution must be truncated because $0 \leq \overline{\beta}_o \leq 1$. Therefore, $\overline{\beta}_o$ for an MS at distance of r

TABLE II

PARAMETERS DEFINING $\mu(r)$

Environment	a_1	a_2	γ [m]	RMS error in $\mu(r)$
GTU	0.599	0.509	329.6	0.004
GBU	0.608	0.424	372.6	0.007

can be approximated by

$$\overline{\beta}_o = \begin{cases} \mu(r) + \sigma\eta, & -\frac{\mu(r)}{\sigma} \leq \eta \leq \frac{1-\mu(r)}{\sigma} \\ 0, & \text{otherwise} \end{cases}, \quad (4)$$

where η is a zero-mean, unit-variance, Gaussian random variable, $\sigma = 0.179$, and $\mu(r)$ is a monotonically increasing function of r. Truncating the distribution in such a manner skews the first and second moments of $\overline{\beta}_o$. However, the distortion introduced is negligible as the observed values of the two limits, $\mu(r)/\sigma$ and $(1 - \mu(r))/\sigma$, are at least of the order of 2 for $r \geq 200$ m.

Figure 6 plots the observed $\mu(r)$ for the two environments. It also plots the minimum-mean-square-error parametric curve-fit of the form:

$$\mu(r) = a_1 - a_2 \exp(-r/\gamma). \quad (5)$$

It can be seen that the empirical curve-fit is accurate. As expected, $\mu(r)$ for GBU is greater than that for GTU, for a given r. The functional form also satisfies the intuitive requirement that it should be monotonically increasing and should saturate for large r. Table II lists the values derived for a_1, a_2, and γ for the two environments. Note that these results have a functional form different from the one proposed in [12], in which the median value of the time-averaged OF varied as $\frac{kr}{1+kr}$, where $k = 0.0029/\text{m}$ for $\epsilon = 0.5$.

IV. CONCLUSIONS

We evaluated the statistics of the time-averaged orthogonality factor, $\overline{\beta}_o$, seen at different locations in an urban macro-cellular area. The ensemble of channel delay profiles obtained from the general and comprehensive COST259 channel model for macrocells was used for this purpose. As COST259 brings a vast amount of work on channel modeling and measurements into a single general framework, it enables us to make general observations and conclusions about the behavior of the OF in a cellular area. Another reason for using COST259 is that it explicitly models the distance-dependence of delay decay constant and the presence of multiple clusters. Both of these have a significant impact on the OF.

In both the Generalized Typical Urban environment and the more dispersive Generalized Bad Urban environment, which are defined in COST259, the value of $\overline{\beta}_o$ was found to vary over a wide range of values even for a given distance of the mobile station from the base station. In general, it increased with distance. This suggests that using a single value for the OF in downlink capacity calculations and simulations might lead to misleading conclusions. We also showed that the time-averaged OF can be modeled as a truncated Gaussian random variable with a distance-dependent mean and a distance-independent standard deviation. Consequently, $\overline{\beta}_o$ can now be generated directly without having to set up the general, but complex, COST259 macrocellular channel model.

REFERENCES

[1] H. Holma and A. Toskala, *WCDMA for UMTS*. John Wiley, 2000.

[2] K. Sipilä, Z.-C. Honkasalo, J. Laiho-Stefens, and A. Wacker, "Estimation of capacity and required transmission power of WCDMA downlink based on a downlink pole equation," in *Proc. VTC*, pp. 1002–1005, 2000.

[3] K. Hiltunen and B. De Ricardo, "WCDMA downlink capacity estimation," in *Proc. VTC*, pp. 992–996, 2000.

[4] X. Qiu, L. F. Chang, Z. Kostic, T. M. Willis, III, L. J. Greenstein, N. B. Mehta, K. Chawla, J. F. Whitehead, and J. Chuang, "Some performance results for the downlink shared channel in WCDMA," in *Proc. ICC*, pp. 376–380, 2002.

[5] N. B. Mehta, L. J. Greenstein, T. M. Willis, III, and Z. Kostic, "Analysis and results for the orthogonality factor in WCDMA downlinks," *IEEE Trans. Wireless Commun.*, pp. 1138–1149, 2003.

[6] O. Awoniyi, N. Mehta, and L. Greenstein, "Characterizing the orthogonality factor in WCDMA downlinks," *IEEE Trans. Wireless Commun.*, vol. 2, pp. 621–625, 2003.

[7] L. Greenstein, V. Erceg, Y. Yeh, and M. Clark, "A new path-gain/delay-spread propagation model for digital cellular channels," *IEEE Trans. Veh. Technol.*, vol. 46, pp. 477–485, 1997.

[8] A. Algans, K. I. Pederson, and P. E. Morgensen, "Experimental analysis of joint statistical properties of azimuth spread, delay spread, and shadow fading," *IEEE J. Select. Areas Commun.*, vol. 20, pp. 523–531, 2002.

[9] U. Martin, "Spatio-temporal radio channel characteristics in urban macrocells," in *IEE Proc. Radar, Sonar and Navigation*, pp. 42–49, 1998.

[10] A. Kuchar, J. P. Rossi, and E. Bonek, "Directional macro-cell channel characterization from urban measurements," *IEEE Trans. Antennas Prop.*, vol. 48, pp. 137–146, 2000.

[11] A. F. Molisch, H. Asplund, R. Heddergott, M. Steinbauer, and T. Zwick, "The COST259 directional channel model - I. overview and methodology," *Submitted to IEEE Trans. Wireless Commun.*

[12] K. I. Pederson and P. E. Mogensen, "The downlink orthogonality factors influence on WCDMA system performance," in *Proc. VTC (Fall)*, pp. 2061–2065, Sept. 2002.

[13] C. Passerini and G. Falciasecca, "Modeling of orthogonality factor using ray-tracing predictions," *IEEE Trans. Wireless Commun.*, vol. 3, pp. 2051–2059, Nov. 2004.

[14] C. Passerini and G. Falciasecca, "Correlation between delay-spread and orthogonality factor in urban environments," *Electron. Lett.*, vol. 37, pp. 384–386, Mar. 2001.

[15] M. Humukumbure, M. Beach, and B. Allen, "Downlink orthogonality factor in UTRA FDD systems," *Electron. Lett.*, vol. 38, pp. 196–197, Feb. 2002.

[16] H. M. El-Sallabi, J. Sallo, and P. Vainikainen, "Investigations on impact of bandwidth on orthogonality factor for WCDMA systems," in *Proc. WCNC*, pp. 1138–1142, Mar. 2004.

[17] M. Steinbauer and A. F. Molisch, "Directional channel modelling," in *Wireless Flexible Personalised Communications. COST259: European Co-operation in Mobile Radio Research* (L. M. Correia, ed.), ch. 3.2, John Wiley, 2001.

[18] "Spatial channel model for multiple input multiple output (MIMO) simulations," Tech. Rep. 25.996, 3rd Generation Partnership Project.

[19] K. Kalliola, J. Laurila, M. Toeltsch, K. Hugl, P. Vainikainen, and E. Bonek, "3-D directional wideband dual-polarized measurement of urban mobile radio channel with synthetic aperture technique," in *Proc. AP2000*, 2000.

[20] A. A. Glazunov, H. Asplund, and J.-E. Berg, "Statistical analysis of measured short-term impulse response functions of 1.88 GHz radio channels in Stockholm with corresponding channel model," in *Proc. VTC*, pp. 107–111, 1999.

[21] *COST 207: Digital Land Mobile Radio Communications (Final Report)*. COST 207 Management Committee, 1989.

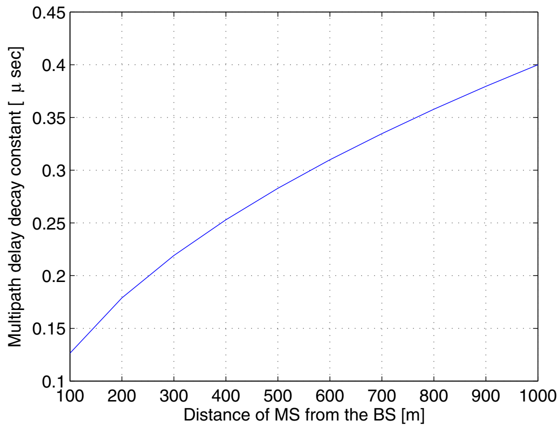

Fig. 1. Median multipath delay time constant of the first cluster as a function of the distance of the MS from the BS (in meters) (same for GTU and GBU)

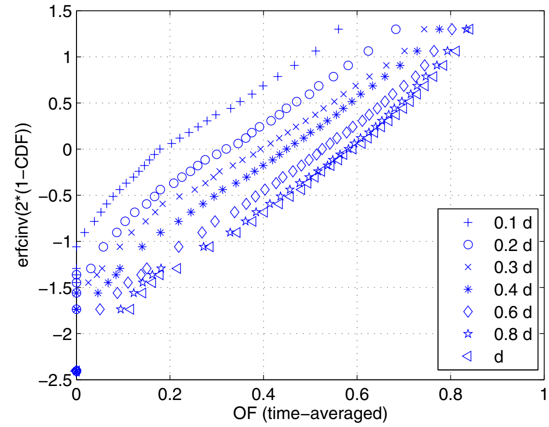

Fig. 4. Generalized Typical Urban environment: CDF of $\overline{\beta}_o$ plotted on 'Gaussian probability scale' for different distances

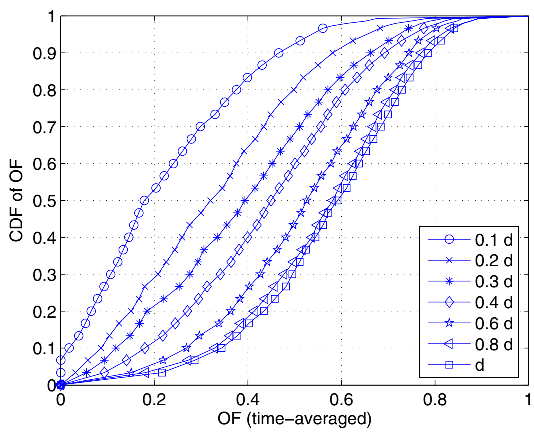

Fig. 2. Generalized Typical Urban environment: CDF of $\overline{\beta}_o$ as function of distance, r (in meters), from base station

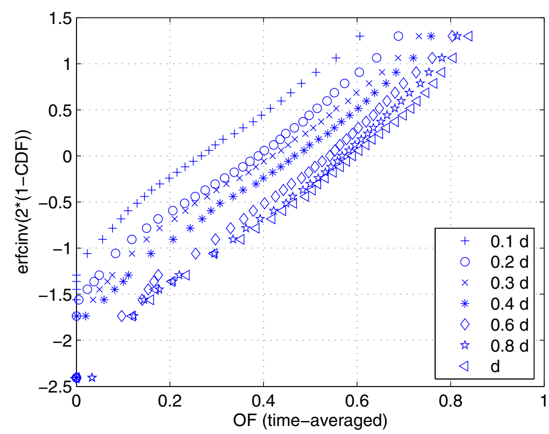

Fig. 5. Generalized Bad Urban environment: CDF of $\overline{\beta}_o$ plotted on 'Gaussian probability scale' for different distances

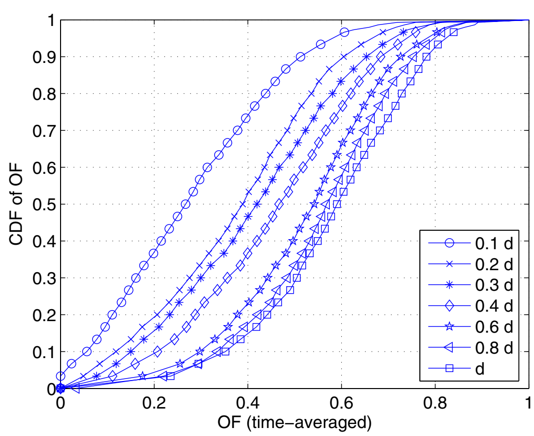

Fig. 3. Generalized Bad Urban environment: CDF of $\overline{\beta}_o$ as a function of distance, r (in meters), from base station

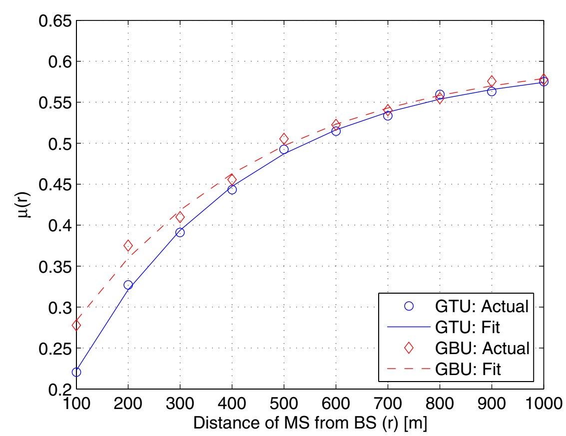

Fig. 6. Mean (μ) as a function of r [m] for GTU and GBU